PERGAMON

Deep-Sea Research II 48 (2001) 4081–4100

DEEP-SEA RESEARCH
PART II

www.elsevier.com/locate/dsr2

Phytoplankton pigment distribution in relation to silicic acid, iron and the physical structure across the Antarctic Polar Front, 170°W, during austral summer

C. Mengelt[a,*], M.R. Abbott[b], J.A. Barth[b], R.M. Letelier[b], C.I. Measures[c], S. Vink[c]

[a] *Department of Ecology, Evolution and Marine Biology, University of California, Santa Barbara, CA 93106, USA*
[b] *College of Oceanic and Atmospheric Sciences, Oregon State University, USA*
[c] *Department of Oceanography, University of Hawaii, USA*

Received 12 April 2000; received in revised form 22 September 2000; accepted 3 January 2001

Abstract

In order to study the factors controlling the phytoplankton distribution across the Antarctic Polar Frontal Region (PFR), surface pigment samples were collected during austral summer (January/February 1998) near 170°W. Both the Polar Front (PF) and the Southern Antarctic Circumpolar Current Front (SACCF) were regions of enhanced accumulation of phytoplankton pigments. The mesoscale survey across the PF revealed two distinct phytoplankton assemblages on either side of the front. The phytoplankton community was dominated by diatoms south of the PF and by nanoflagellates (primarily by prymnesiophytes) to the north. Surprisingly, chlorophyll *a* concentrations did not correlate with mixed-layer depths. However, an increase of the dominance of diatoms over prymnesiophytes was observed with decreasing mixed-layer depths. Despite this relationship, we conclude that the average light availability in the mixed layer was not an important factor influencing the shift in phytoplankton composition across the PF. Although no correlation was found between the surface distribution of the major phytoplankton taxa and dissolved iron or silicic acid concentrations, the location of the strongest vertical gradient in silicic acid and iron concentration coincides with the maximum abundance of diatoms. We conclude that the difference in taxonomic composition is a result of increased silicic acid and iron flux to the upper mixed layer as a result of the increased vertical gradient of these key nutrients south of the front.

1. Introduction

With growing concerns about the impact of elevated atmospheric carbon dioxide (CO_2) on the global climate, international effort has been increased to understand the role of the ocean in the

*Corresponding author. Tel.: +1-805-893-4319; fax: +1-805-893-4319.
E-mail address: mengelt@lifesci.ucsb.edu (C. Mengelt).

0967-0645/01/$ - see front matter
PII: S0967-0645(01)00081-9

CO_2 cycle (Longhurst, 1991; Berger and Wefer, 1991; Boden et al., 1994; Keeling et al., 1996). In particular, regions of bottom water formation such as the North Atlantic and the Southern Ocean have the potential to be a net sink for atmospheric CO_2 (Knox and McElroy, 1984; Martin et al., 1990). Biological activity can increase the net sequestration of CO_2 by photosynthetically converting CO_2 into organic carbon, and by the subsequent formation of larger, fast sinking aggregates that transport the carbon into the interior of the ocean (Berger and Wefer, 1991; Peng and Broecker, 1991; Sarmiento and Orr, 1991). This process is referred to as the biological pump. Diatoms, due to their increased size, tend to be grazed upon by larger zooplankton, which excrete fast sinking fecal pellets resulting in a more efficient biological pump compared to smaller algal species (Dugdale and Goering, 1967; Silver and Gowing, 1991; Dugdale et al., 1995).

Besides being an area of bottom water formation, the Southern Ocean is also of interest because of the high concentrations of nitrate and phosphate contrasting the low phytoplankton biomass. It is an ongoing debate whether the low biomass in this high nutrient low chlorophyll (HNLC) region can be attributed to iron limitation, light limitation, or grazing (Holm-Hansen et al., 1977; Martin et al., 1990; Nelson and Smith, 1991; Tréguer and Jacques, 1992; Banse, 1996). Recent studies have identified both iron and silicic acid as key nutrients affecting the biological pump in the Southern Ocean (De Baar et al. 1995, 1999; Franck et al., 2000). De Baar et al. (1999) have shown that diatom growth north of the Polar Frontal Region (PFR) is limited both by low silicic acid and iron availability. In addition, upwelling of silicate rich deep water onto the continental shelf correlates with increased diatom biomass (Prézelin et al., 2000). Silicic acid availability enhances diatom growth, and will hence increase the efficiency of the biological pump. On the other hand, increased iron availability is considered to decrease the extent of the Southern Ocean HNLC region, and therefore suggested to increase the flux of organic carbon to the sediments (Martin et al., 1990). The sequestration of atmospheric CO_2 is therefore enhanced by silicic acid as a result of a change in the pelagic community structure, and by iron as a result of increased carrying capacity of the ecosystem.

The heterogeneous nature of the Southern Ocean results in differences in the magnitude and the controls of phytoplankton abundance and productivity (Moore and Abbott, 2000). Our study covered three ecologically distinct regions: The PFR, the Permanently Open Ocean Zone (POOZ), and the Seasonal Ice Zone (SIZ) (Tréguer and Jacques, 1992; Moore and Abbott, 2000). The PFR is defined as the area within 1° latitude north and south of the Polar Front (PF). The PF is the location of a strong horizontal gradient in temperature and salinity (Orsi et al., 1995). It is associated with an intensified eastward current and strong mesoscale meandering. The meandering is also associated with areas of upwelling (cyclonic bend of the meander) and downwelling (anti-cyclonic bend) (Flierl and Davis, 1993; Barth et al., 2001). The variability associated with the meandering of the jet will hence influence the environment for phytoplankton growth by varying the upwelling rate of nutrients. In fact, satellite images (Moore and Abbott, 2000) indicate enhanced phytoplankton biomass at the PF. Consistent with that observation, high chlorophyll *a* (chl *a*) biomass was observed downstream of a cyclonic meander, where nutrient upwelling is expected, during an earlier cruise in November/December 1997 (Barth et al., 2001). An analog to the PF is the Southern Antarctic Circumpolar Current Front (SACCF), marking the southern extent of the Antarctic Circumpolar Current (ACC), which also appears to be a location of elevated

biomass (Moore and Abbott, 2000). The POOZ extends south of the PFR to the SIZ and is typically an area of consistent low phytoplankton biomass. The SIZ is defined as the area covered with $>5\%$ ice cover during the winter prior to the growing season and $<70\%$ ice cover during the summer (seasonal minimum ice extent). The SIZ is generally a very productive area, since stratification from recently melted ice decreases the mixed-layer depths and allows for large blooms (Smith and Nelson, 1985, 1990). Near 170°W the SIZ extends almost as far north as the PFR due to a southward bend of the PF (Moore and Abbott, 2000). As a result, the extent of the POOZ is minimal, which allows for bloom favorable conditions associated with the melting of the seasonal ice to span almost the entire region between the continental shelf and the PFR along 170°W.

The purpose of the US Joint Global Ocean Flux Study (JGOFS) in the Southern Ocean was to gain insight into the magnitude and the controls of carbon flux in the open ocean region of the Southern Ocean (Smith et al., 2000). Due to the effect of phytoplankton species on the efficiency of the biological pump, we were interested in identifying the dominant phytoplankton groups. Our goal was also to determine the physical or chemical factors (e.g. mixed-layer depths, silicic acid or iron distribution) controlling the taxonomic composition of phytoplankton in the PFR and the ACC during austral summer. The strong gradient in hydrography across the PF makes the site an ideal location to study the controls regulating the dominance of different phytoplankton groups.

2. Material and methods

2.1. Sample collection

Pigment samples were collected aboard the R/V *Roger A. Revelle* during January 8–February 8, 1998. The first sampling period was during the southbound transect, January 13–16, along 170°W from 56–68°S (Fig. 1.). Five days later, the PF was surveyed twice (January 21–25 and January 30–February 3). The two surveys at the PF were centered on 170°W and extended from 169.4 to 171.9°W and from 60 to 61.6°S (Fig. 1). The sample collection occurred during the same period as SeaSoar surveys along the ship track, every 0.2° latitude and 0.4° longitude (equal to 22 km north–south and $\sim$25 km east–west). Water samples were collected from the ship's surface seawater intake system at approximately 4 m depth. Duplicate 21 aliquots were filtered onto GF/F Whatman filters. Filters were frozen and stored in -80°C freezer until analyzed on shore.

2.2. Sample analysis

Samples were extracted in 3 ml of 100% acetone with the addition of 0.1 ml of internal standard canthaxanthin, sonicated for 90 s, and extracted for 12 h at -20°C. They were then pre-concentrated by evaporation under constant flow of nitrogen for 10 min. Phytoplankton pigment concentrations were determined using a high-performance liquid chromatography (HPLC) system composed of a Perkin–Elmer pump, an Ultrasphere analytical column (150 mm $\times$ 4.6 mm), and a SpectraSystem UV2000 absorption detector (dual wavelength, at 436 and 665 nm). The mobile

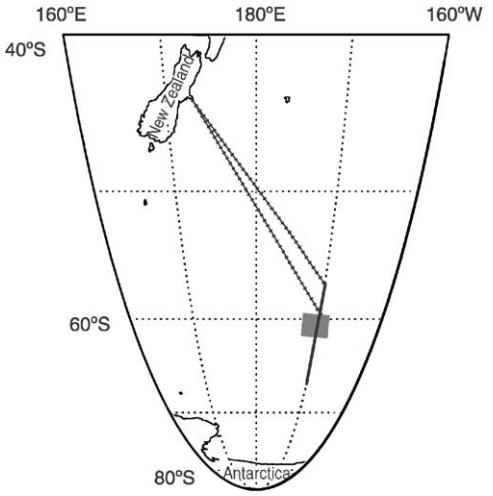

Fig. 1. Location of the cruise aboard the R/V *Revelle* during January/February 1998. Bold black line indicates the location of sample collection along the southbound transect. The gray shaded area marks the location of the two mesoscale surveys.

solvent system method was adapted from Wright and Jeffrey (1997). The instrument was calibrated using commercial pigment standards (Sigma Chemicals and VKI, Denmark). The detection limit for the pigment concentrations was $0.005\,\mu g\,l^{-1}$. Chl *a* concentrations were used to estimate phytoplankton biomass and chlorophyllide *a* (chlide *a*) concentrations were determined as a possible indicator for senescent phytoplankton, particularly damaged diatoms (Jeffrey et al., 1997). Chlide *a* concentrations in a sample could increase as a result of degradation during the extraction. However, extractions were done in 100% acetone to minimize degradation and the same extraction procedure was used for all samples. Therefore, we would expect a constant percentage of chl *a* degradation. The following carotenoids were used as marker pigments to determine the taxonomic composition: fucoxanthin (fuco) for diatoms, 19′-hexanoyloxyfucoxanthin (hex) for prymnesiophytes, 19′-butanoyloxyfucoxanthin (butanoyl) for chrysophytes, peridinin (peri) for dinoflagellates, alloxanthin (allo) for cryptophytes, and chlorophyll *b* (chl *b*) for chlorophytes (Jeffrey and Vesk, 1997; Bidigare et al., 1996). Fuco also has been found in the prymnesiophyte *Phaeocystis* spp. (Wright and Jeffrey; 1987; Buma et al., 1991; Vaulot et al., 1994). However, *Phaeocystis* is predominantly associated with ice-edge blooms and rarely observed offshore (Fryxell and Kendrick, 1988; Bidigare et al., 1996). Fuco is also found in three species of dinoflagellates (Jeffrey et al., 1975), however, microscopic observations confirm the dominance of diatoms at 61°S (Brown and Landry, 2001). Therefore, we assume that fuco is a marker pigment specific to diatoms for the time and location of our study. Pigment data were interpolated linearly to generate the contour plots with a grid spacing of 0.05° longitude and 0.1° latitude. Pigment concentrations at the surface were assumed to be representative of the average concentrations within the upper mixed layer based on the fact that seven of the eight vertical pigment profiles (Goericke, unpublished) revealed a uniform depth distribution of the major pigments within the upper mixed layer.

2.3. Physical data and mixed-layer depths

The conductivity, temperature and depth (CTD) data were collected by a SeaSoar cycling from 0 to 400 m every 8–10 min. Details of data collection and processing are described in Barth and Bogucki (2000) and Barth et al. (2001). The mixed-layer depth (MLD) is defined as the depth at which the density anomaly differs by 0.01 $kg\,m^{-3}$ from its surface value (Brainerd and Gregg, 1995). Shipboard Acoustic Doppler Current Profiler (ADCP) velocities were obtained in 8 m bins, down to 300–350 m depending on sea state every 2.5 min, using a hull-mounted 153.6 kHz narrow-band RD Instruments system (Barth et al., 2001). Water velocity relative to the earth was obtained by subtracting the ship's motion computed by time-differencing the P-Code GPS ship location.

2.4. Iron data

Surface samples ($\sim$1 m depth) were collected from a "fish" towed by a boom extended approximately 4 m outboard from the aft quarter of the ship (Vink et al., 2000). Surface water was pumped peristaltically on board through Teflon-lined polyethylene tubing. The outlet of this tubing was passed into a plastic tent mounted over a sink. Discrete samples for determination of total dissolved iron (Fe) were collected from this outlet while the ship was underway. These samples were filtered in a class 100 flow bench through a 0.2-μm acid-leached Gelman acro-50A filter.

Vertical profile samples were collected from either Go-Flo bottles mounted on a trace metal clean rosette or from Niskin bottles mounted on a resin-coated clean rosette. No significant or systematic differences were found between results obtained from these different sampling systems. These samples were also filtered in a class 100 flow bench through the same 0.2-μm filters as the underway samples. Iron concentrations were determined using the method of Measures et al. (1995). Samples were pre-concentrated in-line for 3 min onto a resin of immobilized 8-hydroxyquinoline (Landing et al., 1986). Iron concentrations were determined by the spectrophotometric detection of dimethyl-p-phenylenediamine dihydrochloride (DPD) oxidized by Fe. Standards were made by addition of known amounts of Fe standard (Fisher Scientific) to filtered, acidified seawater collected underway. The technique had a precision of 3–4% during this cruise.

2.5. Silicic acid data

Surface H_4SiO_4 data were collected using the pump described above and measured using the high-sensitivity acid-molybdate method (Brzezinski and Nelson, 1989). The precision of this method is $\pm 1\%$ or $\pm 0.05\,\mu M$, whichever is greater. H_4SiO_4 profile data were obtained from regular CTD rosette and analyzed following JGOFS protocols (JGOFS, 1996) using a 5-channel Technicon II AA system.

3. Results

3.1. Southbound transect along 170°W

3.1.1. Position of the fronts

During the transect, the steepest surface temperature gradient was observed between 61°S and 61.2°S, consistent with the position calculated from AVHRR satellite SST data (Moore et al.,

1999). The center of the intensified eastward jet was observed around 61.1°S (Barth and Cowles, in preparation). This agrees well with the observation on the spring cruise 1997, where the center of the eastward jet was positioned just north of the steepest temperature gradient (Barth et al., 2001). The position of the SACCF was observed between 64.5°S and 65°S, corresponding with the position of intensified eastward jet associated with that front (Barth and Cowles, in preparation).

3.1.2. Phytoplankton pigment distribution

Surface chl *a* concentrations measured during the southbound transect yielded two local maxima, one at the PF and one near the SACCF (Fig. 2a). At the latter, chl *a* reached values as high as $0.7\,\mu g\,l^{-1}$. Chlide *a* concentrations was also highest at the location of the SACCF (Fig. 2b). The ratio of chlide *a* to chl *a* was significantly higher (0.9) at the SACCF compared with ratios around 0.4 for the rest of the transect. This increase could be both a function of grazing or senescence of the diatom bloom. Microscopic observations support the latter reason (Brown and Landry, 2001). The chl *a* measurements based on HPLC are consistently lower (as much as 50% lower) than the chl *a* concentrations measured by fluorometry. The same discrepancy is also seen between the HPLC chl *a* measurements from another lab. (Goericke, unpublished) and the fluorometric chl *a* measurements. Both data sets have been vigorously checked for systematic errors and the discrepancy seems to be inherent in the different methods. Therefore, it is important to consider these estimates of phytoplankton biomass as rather conservative. In addition, our method was not able to resolve all of the chl *a* allomers, and therefore we only report chl *a* and not total chl *a*, which is the sum of all the allomers, chlide *a* and chl *a*. Only on the transect did chlide *a* concentrations reach high enough concentrations worth mentioning. We therefore report both chl *a* and chlide *a* for the transect only. Maximum fuco concentrations were $1\,\mu g\,l^{-1}$ (Fig. 2c) and hex reached $0.23\,\mu g\,l^{-1}$ (Fig. 2d). These pigments displayed a meridional distribution similar to that observed for chl *a*, with increased concentrations at the two physical fronts. However, north of the PF hex was more abundant than fuco, which was reflected in the low fuco : hex ratio (Fig. 2e). The remaining pigments peri, butanoyl, and allo (marker pigments for dinoflagellates, chrysophytes, and cryptophytes, respectively) also showed a trend of increased concentrations near the PF and the SACCF, but their maximum concentrations were low compared to hex and fuco (Fig. 2f). Throughout the entire ACC region south of the PF, diatoms appeared to dominate the phytoplankton assemblage, with the fuco : (peri + butanoyl + hex + allo) ratio > 1 (not shown). North of the PF this ratio was less than one, suggesting that nanoflagellates, prymnesiophytes in particular, dominated the phytoplankton assemblage.

Fig. 2. Pigment concentration for surface samples collected during the southbound transect along 170°W. The shaded areas indicate the location of the Antarctic Polar Frontal Region (PFR) and the Southern Antarctic Circumpolar Current Front (SACCF). Error bars indicate one standard deviation. The following pigments are shown: (A) chlorophyll *a* concentration ($\mu g\,l^{-1}$); (b) chlide *a* concentration ($\mu g\,l^{-1}$) c) fucoxanthin concentration ($\mu g\,l^{-1}$), which is a marker pigment for diatoms; (d) 19′-hexanoyloxyfucoxanthin concentration ($\mu g\,l^{-1}$), which is a marker pigment for prymnesiophytes; (e) the ratio of fucoxanthin to 19′-hexanoyloxyfucoxanthin (wt : wt), as an estimate of the dominance of either group; (f) Peridinin indicated by crosses (x), 19′-butanoyloxyfucoxanthin indicated by closed diamonds (◆) and alloxanthin concentration indicated by open circles (○) ($\mu g\,l^{-1}$). The dashed line in (e) marks the 1 : 1 ratio.

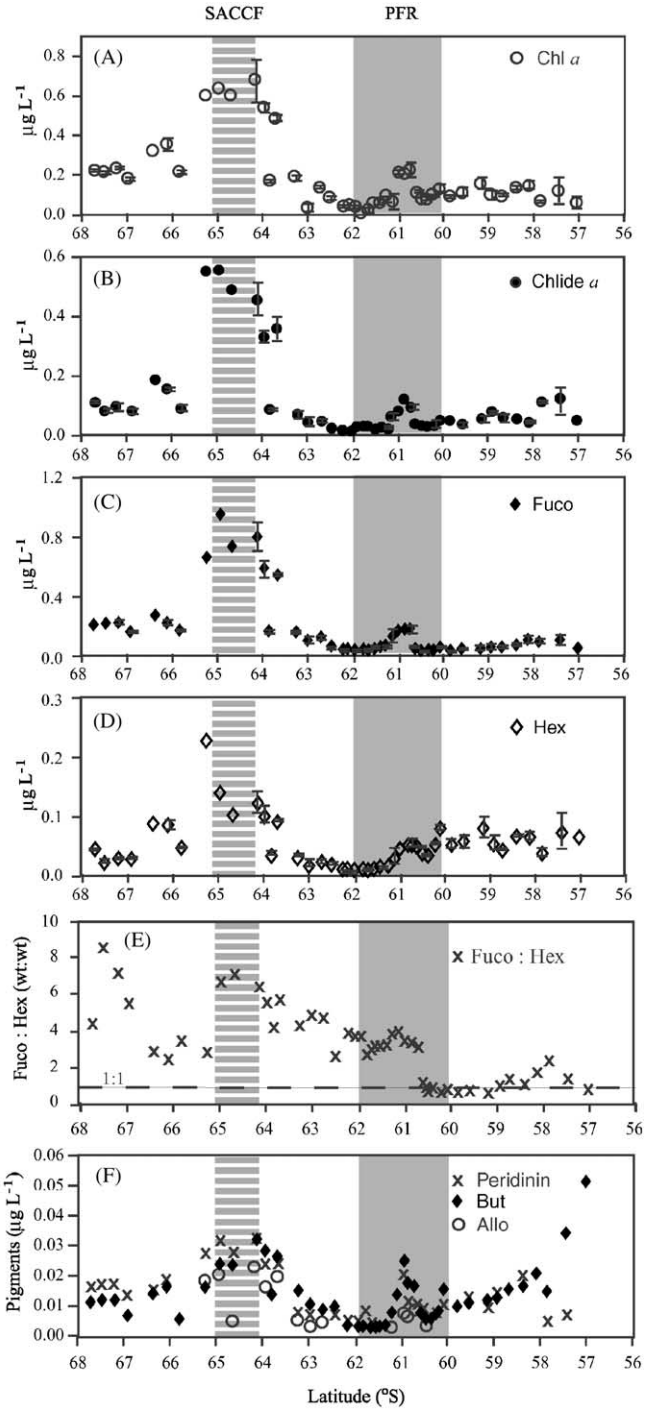
SACCF
PFR
(A)
Chl a
(B)
Chlide a
(C)
Fuco
(D)
Hex
(E)
Fuco : Hex
1:1
(F)
Peridinin
But
Allo
µg L-1
Fuco : Hex (wt:wt)
Pigments (µg L-1)
Latitude (°S)

3.1.3. Nutrient distribution

Nitrate and phosphate concentrations were high throughout our study area. Nitrate concentrations in the upper mixed layer never declined below 18 μM, and phosphate was always greater than 1 μM. Surface silicic acid concentrations measured during the transect were very low (<3 μM) north of the meridional H_4SiO_4 gradient at 65°S, where surface concentrations increased to >50 μM, with the exception of higher and more variable values in the PFR, ranging from 1 to 6.5 μM (Fig. 3). This meridional gradient resulted from biological draw-down of H_4SiO_4 in the region between the H_4SiO_4 gradient and the PFR by elevated biomass observed in spring and early summer (Brzezinski et al., 2001; Nelson et al., 2001). Similarly, iron concentrations were elevated within the PFR relative to adjacent waters and increased just south of the SACCF (Fig. 3). However, increased iron concentrations also were observed between 63.5°S and 65°S where surface waters were depleted in H_4SiO_4.

3.2. Mesoscale surveys of the Polar Frontal Zone at 170°W

3.2.1. Physics across the Polar Front

Surface temperatures were about 2°C higher than observed during spring throughout the survey area (Barth and Cowles, in preparation). Both mesoscale surveys revealed a surface water temperature gradient of 1.7°C per degree latitude, with surface temperature dropping from 5°C to 2.5°C between 60°S and 61.5°S (Barth and Cowles, in preparation). Horizontal velocities, based on ADCP data, were maximal in a relatively narrow band centered in the region of the strongest meridional temperature gradient (near 61.1°S). They were primarily eastward and reached values of 0.25 m s^{-1} during the first survey and somewhat higher values during the second survey (Barth and Cowles, in preparation). Currents revealed only weak meandering, in contrast to observations during a spring cruise (Barth et al., 2001; Abbott et al., 2000). Drifters were released within the center of this jet during the first mesoscale survey (Abbott et al., 2001). These drifters stayed well

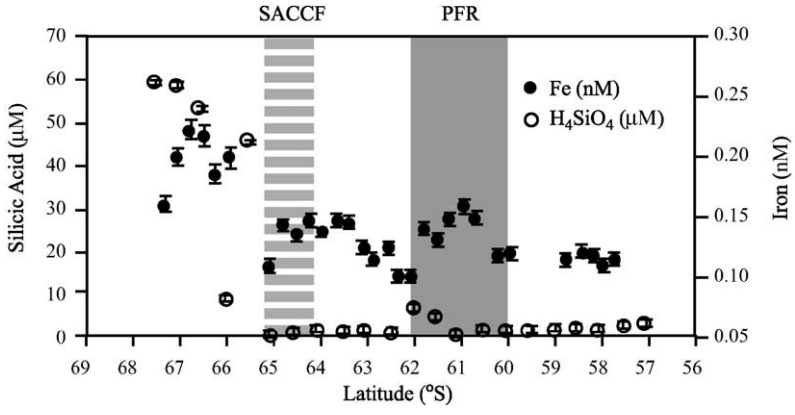

Fig. 3. Silicic acid (μM) and iron (nM) concentrations for surface samples collected during the southbound transect along 170°W. The shaded areas indicate the location of the Antarctic Polar Frontal Region (PFR) and the Southern Antarctic Circumpolar Current Front (SACCF). Error bars on the iron data indicate the 4% error and on the silicic acid data the 1% error (or ± 0.05 μM, whichever is larger) associated with each method.

within the center of the jet and for the purpose of the following discussion, the drifter tracks are used to mark the PF (Figs. 4 and 5).

3.2.2. Phytoplankton assemblage across the Polar Front

The high resolution survey revealed two areas of elevated chl *a* concentration on either side of the PF (Figs. 4a and 5a). This pattern was more pronounced during the first survey than during the second. Butanoyl concentrations were very low but displayed a similar distribution than chl *a* (Figs. 4b and 5b). Fuco was the most abundant marker pigment south of the front and was significantly higher than hex south of the front during both surveys ($p<0.001$ for both surveys; Wilcoxon rank-sum test) (Figs. 4c and 5c). The concentration of fuco was on average three times higher south than north of the front during the first survey and two times higher during the second survey. Hex was found in highest concentrations north of the PF, with particularly low concentrations south of the PF during the first survey (Figs. 4d and 5d). Allo and peri were present but in very low concentrations (data not shown) on either side of the PF and the other marker pigments were below our detection limit.

3.2.3. Mixed-layer depths and light levels

The mixed-layer depths ranged from 43 to 75 m during the first and from 47 to 83 m during the second SeaSoar survey and were generally deeper north of the PF. A plot of mixed-layer depths and chl *a* reveals no correlation (Fig. 6a and b, $r^2 = 0.02$; Model II regression) during either mesoscale surveys. However, a weak negative correlation can be observed between the mixed-layer depths and the dominance of diatoms over prymnesiophytes (fuco : hex ratio) (Fig. 6c, $r^2 = 0.38$ and Fig. 6d, $r^2 = 0.40$; Model II regression) during both surveys, with slopes significantly different from zero ($p<0.01$ for both surveys). No PAR data were available for this cruise, therefore 1% isolumes were determined based on in situ measured light attenuation coefficients (Cowles, unpublished) in order to assess the influence of light on the species distribution. Only spatially scarce euphotic depth data were available. The 1% isolumes range between 50 and 80 m (Cowles, unpublished), about the same depth range as the mixed-layer depths. Additionally, the shallow mixed layers coincide with the shallower 1% isolumes south of the front. Assuming the surface irradiance was the same, phytoplankton would encounter on average about the same amount of light on either side of the PF if mixed throughout the mixed layer.

3.2.4. Silicic acid and iron across the Polar Front

During both mesoscale surveys surface silicic acid concentrations were low ($<10\,\mu M$) and uniform across the PFR. Surface iron concentrations were elevated compared to adjacent waters and ranged from 0.1 to 0.27 nM Fe and from 0.1 to 0.2 nM Fe during the first and second mesoscale survey, respectively. Nevertheless, the iron concentrations did not correlate with the chl *a* concentrations nor with the fuco : hex ratio. However, silicic acid concentrations below the mixed layer were significantly higher south of the PF at 62°S (36 μM H_4SiO_4; Fig. 7a) compared to north of the PF at 60°S (13 μM H_4SiO_4; Fig. 7c). These higher H_4SiO_4 concentrations at depth resulted in a three-fold higher vertical H_4SiO_4 gradient south of the front compared to that in the north (Table 1). If all other terms are equal, this would result in a three-fold increase in eddy flux of H_4SiO_4 from below the mixed layer (Table 1). In the case of iron, concentrations at depth were only slightly higher south of the front, increasing from 0.16 to 0.25 nM Fe between 60 and 62°S

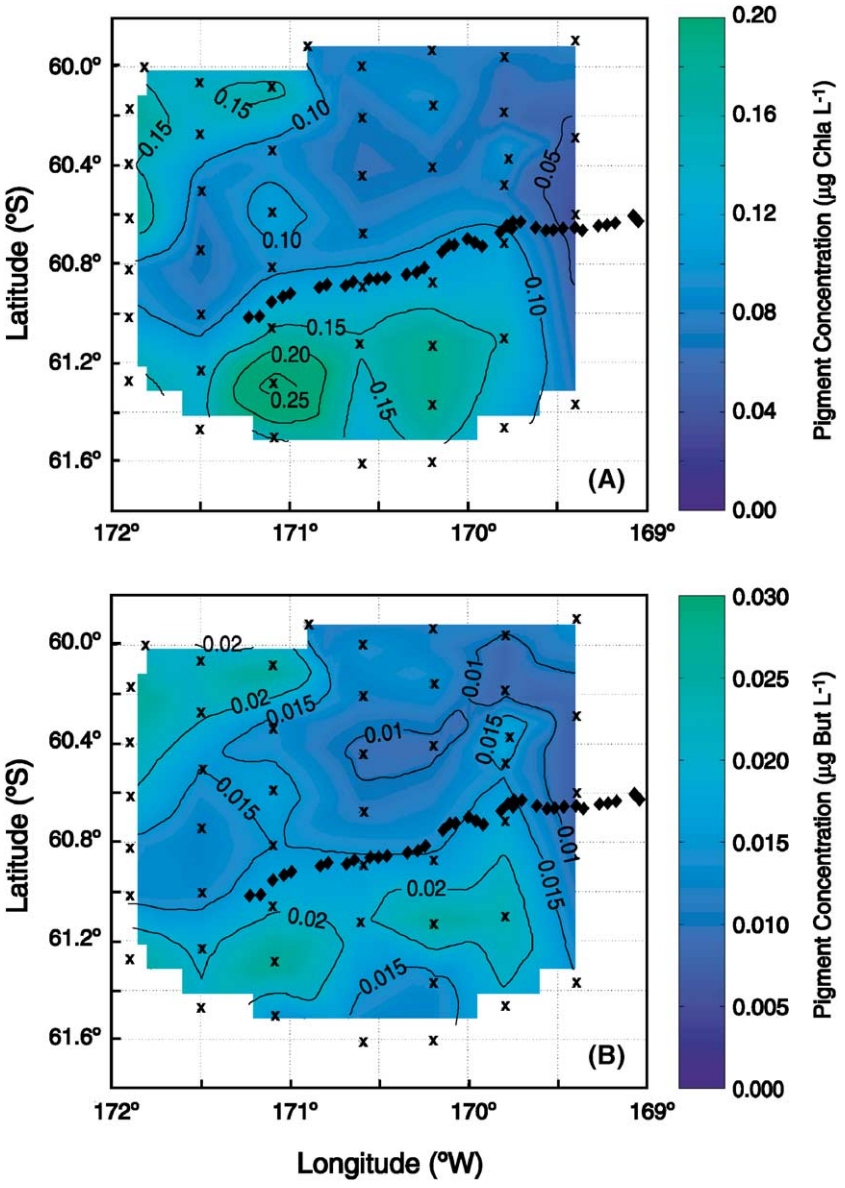

Fig. 4. Pigment concentration for surface samples collected during the first SeaSoar survey at the Polar Front. Crosses indicate the sample location. The black diamonds indicate the position of the Polar Front jet. (a) chlorophyll *a* concentration ($\mu g l^{-1}$); (b) 19′-butanoyloxyfucoxanthin concentration ($\mu g l^{-1}$), which is a marker pigment for prymnesiophytes and chrysophytes; (c) fucoxanthin concentration ($\mu g l^{-1}$), which is a marker pigment for diatoms; (d) 19′-hexanoyloxyfucoxanthin concentration ($\mu g l^{-1}$), which is a marker pigment for prymnesiophytes.

(Fig. 7a and c). The resulting vertical gradient was negative north of the front (-0.33×10^{-3} nM m^{-1}) and positive both within (0.05×10^{-3} nM m^{-1}) and south (0.38×10^{-3} nM m^{-1}) of the front (Table 2). Therefore, any eddy flux north (60°S) of the front

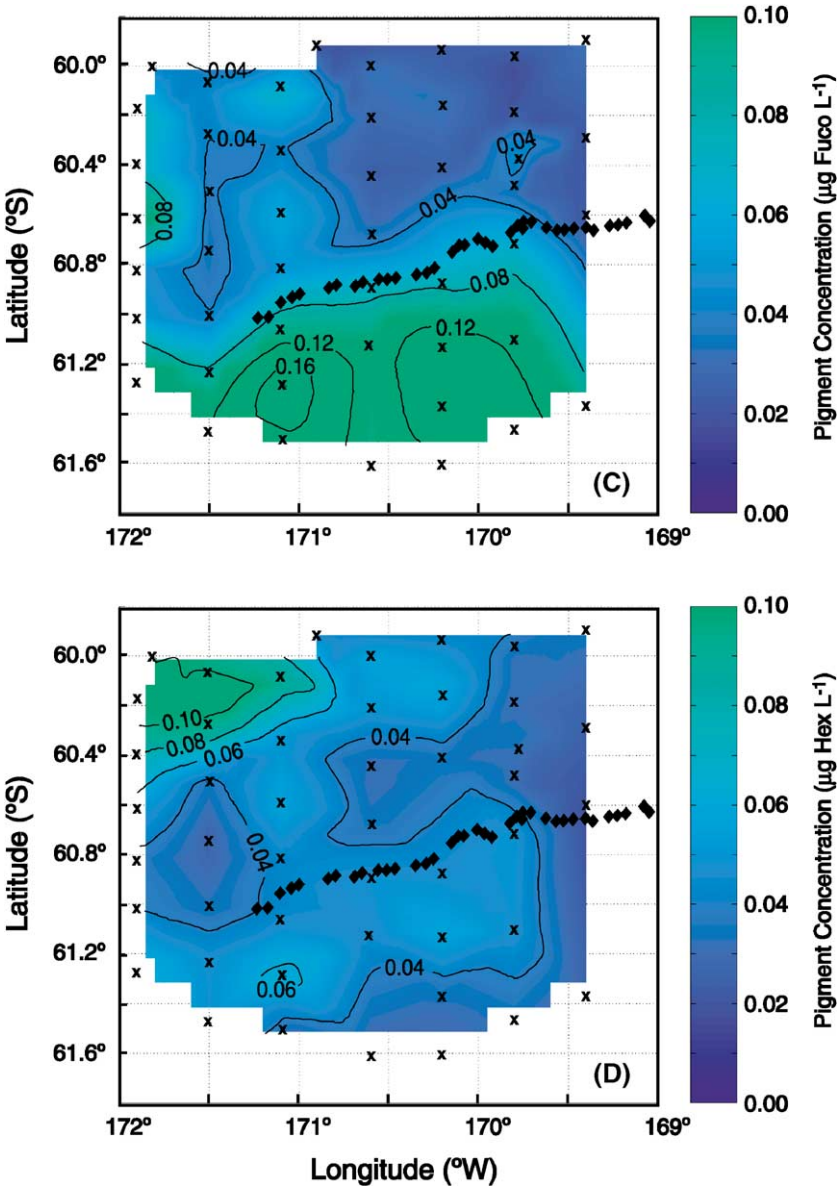

Fig. 4 (*continued*)

would result in a dilution of the measured mixed layer iron concentrations, and in an increase in mixed layer iron concentrations south (62°S) of the front (Table 2).

4. Discussion

During the first PF cruise in austral spring 1997, phytoplankton biomass was generally low except in a small area just south of the PF jet (Barth et al., 2001; Brzezinski et al., 2001). It

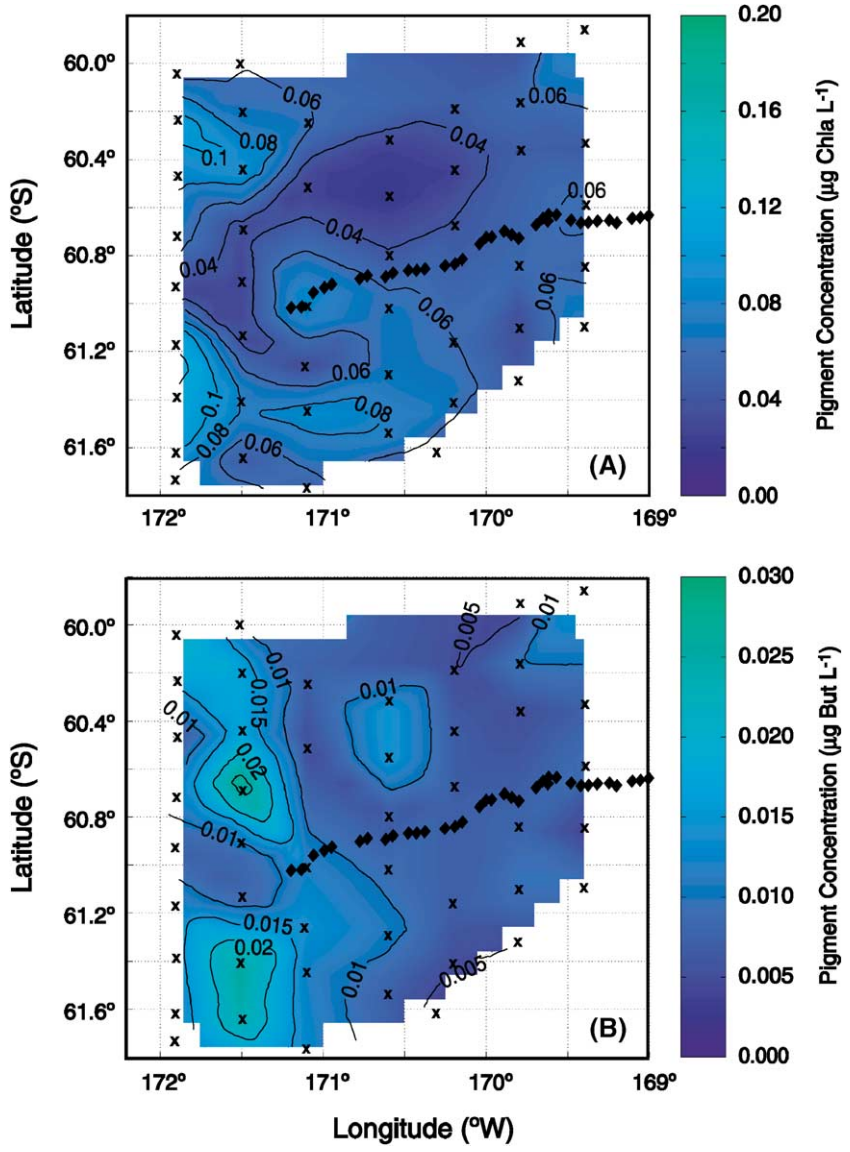

Fig. 5. Same as Fig. 4, but collected during the second SeaSoar survey.

appeared that the onset of stratification in this region facilitated the biomass increase ($>0.8\,\mu g$ chl $a\ l^{-1}$) (Barth et al., 2001). However, the distribution of chl a along the PF was related to mesoscale meandering of the front (Barth et al., 2001), indicating the importance of the meander driven upwelling for the phytoplankton by increasing nutrient and light supply (Abbott et al., 2001). Besides the elevated biomass at the PF, a diatom bloom ($\sim 1.5\,\mu g$ total chl $a\ l^{-1}$; as determined by HPLC; Goericke, unpublished) was observed at around 63–64°S near the retreating ice edge during early summer 1997, and waters immediately north of the bloom were

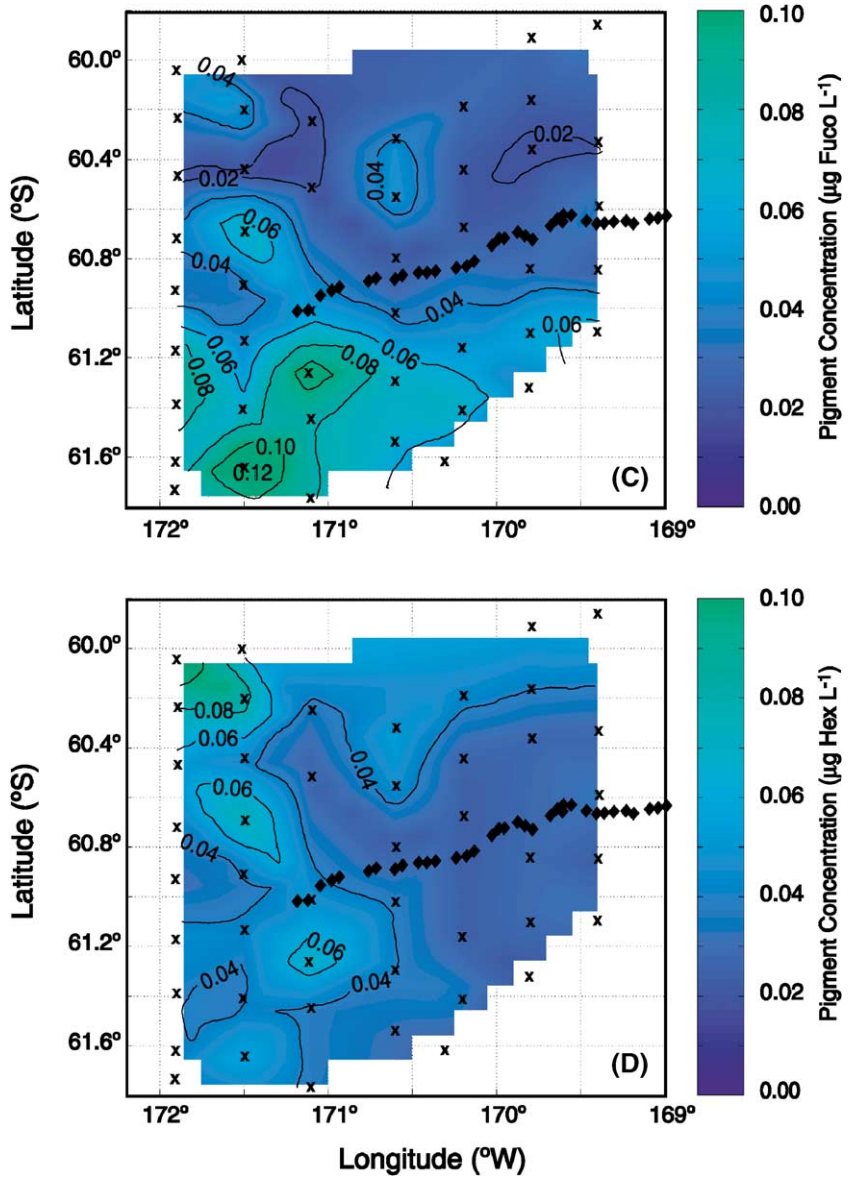

Fig. 5 (*continued*)

depleted in silicic acid (Brzezinski et al., 2001). The large flux into the sediment traps at 63°S (221 mg m^{-2} d^{-1} at 1031 m) was likely a result of this bloom (Honjo et al., 2000).

By the time of our cruise, the strongest meridional surface H_4SiO_4 gradient was within the SACCF (at 65°S) and a bloom (0.8 µg chl *a* l^{-1}; 1.2 µg total chl *a* l^{-1}) was again observed coincident with this gradient. Although chl *a* concentrations were lower (< 1 µg l^{-1}) than typical bloom concentrations, biogenic silica concentrations were high and comparable to concentrations measured in coastal diatom blooms (Brzezinski et al., 1997). The discrepancy between low chl *a*

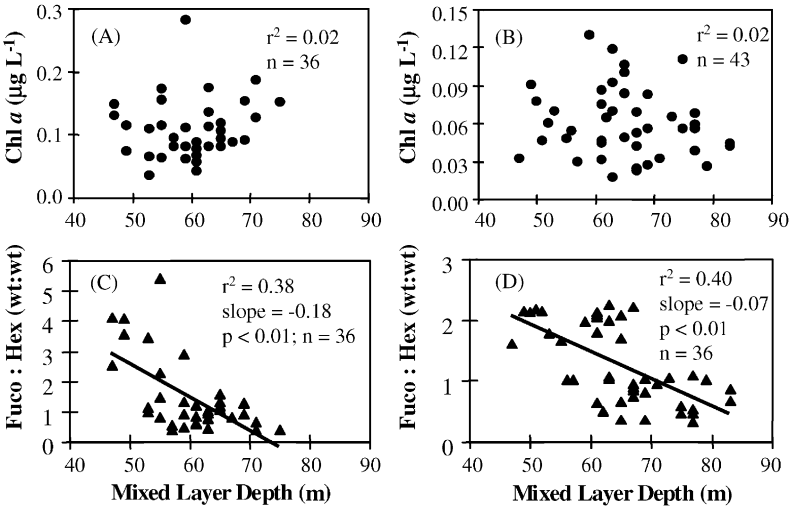

Fig. 6. Relationship between pigments and mixed-layer depths (MLD). (a) and (c) are from the first SeaSoar survey and (b) and (d) from the second survey. (a) and (b) are plots for chlorophyll *a* ($\mu g l^{-1}$) and MLD (m). (c) and (d) are plots for the ratio of fucoxanthin to 19′-hexanoyloxyfucoxanthin and MLD (m), with a linear regression (Model II) fit to each plot.

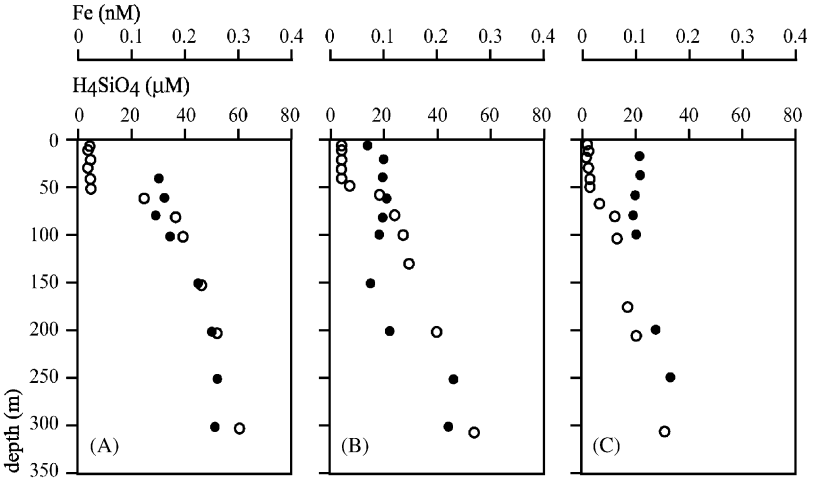

Fig. 7. Vertical profiles for silicic acid (○) (μM) and iron (●) (nM) concentrations from stations along 170°W at (a) 60°S, (b) 61°S, and (c) 62°S.

and high biogenic silicate concentrations could be a sign of a senescent or heavily grazed upon diatom bloom. This would explain the high chlide *a* relative to chl *a* concentrations observed at the location of the bloom. Microscopic observations of abundant empty diatom frustules confirm this speculation (Brown and Landry, 2001). Marker pigments indicate a strong dominance of diatoms within this bloom. The phytoplankton biomass decreased south of the SACCF despite high silicic acid and iron concentrations.

Table 1
Estimates of silicic acid flux based on eddy flux only ($K_z = 3 \times 10^{-5}\,m^2\,s^{-1}$)

	62°S	61°S	60°S
dSi/dz; (mmol m^{-4}) or μM m^{-1}	0.63	0.40	0.19
Eddy flux (mmol $m^{-2}\,s^{-1}$)	1.89×10^{-5}	1.19×10^{-5}	0.56×10^{-5}
Daily flux (mmol $m^{-2}\,d^{-1}$)	1.63	1.03	0.48
Daily production (mmol $m^{-2}\,d^{-1}$)[a]	7.0	4.3	5

[a] Estimate by Brzezinski et al. (2001).

Table 2
Estimates of iron flux based on eddy flux only ($K_z = 3 \times 10^{-5}\,m^2\,s^{-1}$)

	62°S	61°S	60°S
dFe/dz; (μmol m^{-4}) or nM m^{-1}	0.38×10^{-3}	0.05×10^{-3}	-0.33×10^{-3}
Eddy flux (μmol $m^{-2}\,s^{-1}$)	1.15×10^{-8}	0.15×10^{-8}	-1.01×10^{-8}
Daily flux (μmol $m^{-2}\,d^{-1}$)	1.00×10^{-3}	0.13×10^{-3}	-0.87×10^{-3}
Daily production (μmol $m^{-2}\,d^{-1}$)[a]	11.38	6.99	8.13

[a] Estimated using biogenic Si production estimates (Table 1) and average phytoplankton Si : Fe ratios (Collier and Edmond, 1983; Martin and Knauer, 1973; Martin et al., 1976).

With the low surface silicic acid concentrations observed north of 65°S, one would expect the phytoplankton assemblage to shift to groups other than diatoms. However, the dominance of diatoms over prymnesiophytes is relatively constant between the SACCF and the PFR, with the ratio of fuco to the sum of all other pigments declining only two-fold between the SACCF and the PFR. The low ambient iron concentrations and grazing pressure on the smaller autotrophs (Brown and Landry, 2001) could be responsible for the absence of a major shift in the group composition towards non-diatom species.

Despite the depletion of surface H_4SiO_4 north of 65°S, a local maximum in H_4SiO_4 concentration was detected in the PFR on the southbound transect (Fig. 3). Iron concentrations were also slightly elevated in the PFR. The increased iron concentration and the persistent elevated silicic acid concentration at the PFR suggests a re-supply of nutrients from upstream or from below the mixed layer. This re-supply of nutrients in the PFR appears to support higher biomass within the PFR compared to adjacent areas (Fig. 2). Diatoms dominated the assemblage south of the PF but were not an important component of the phytoplankton to the north of the jet, where nanoflagellates were most abundant. However, nanoflagellates were not excluded from the south and contributed on average 22% to the biomass (based on hex and butanoyl biomarkers). Microscopic observations confirm that diatoms dominated also in terms of carbon biomass estimates at the southern edge of the PFR during the transect (Brown and Landry, 2001).

Given the striking differences in phytoplankton assemblage across the PFR, we also would expect to observe a strong meridional gradient in mixed-layer depths, light availability, or nutrient concentrations. Although surface silicic acid and iron concentrations were elevated in the PFR, the concentrations of these dissolved constituents did not correlate with pigment concentrations,

thereby failing to account for the cross-frontal differences in phytoplankton assemblage. Additionally, there was no correlation between the biomass and the mixed-layer depths (Fig. 6). This is surprising, since previous work consistently found increased biomass with shallower mixed layers (Mitchell and Holm-Hansen, 1991; Arrigo et al., 1999; Smith et al., 2000). In most instances, this relationship is a result of increased average irradiance available to the phytoplankton in the mixed layer, which then allows for increased growth. However, this relationship also could be indicative of upwelling of silicic acid and possibly iron allowing for increased diatom biomass (Prézelin et al., 2000). Since we only saw a correlation between the dominance of diatoms over prymnesiophytes and the mixed-layer depths, the relationship is more indicative of increased silicic acid flux than of increased light availability. Additionally, the ratio of the mixed-layer depths to the depth of the 1% isolumes is nearly uniform (around 1) across the front, and does not indicate that light availability was an important factor in structuring the phytoplankton assemblage.

A lack of correlation between the mixed-layer nutrient concentrations and pigment ratios does not necessarily imply that nutrients are not important in controlling the pigment ratios, but rather implies that rates might be more important than concentrations. At low ambient nutrient concentrations, nutrients are likely kept low by biological consumption, and supply rates of those nutrients will control the standing stock and possibly the phytoplankton assemblage (Nelson et al., 1989). The most plausible explanation for the dominance of diatoms south of the PF, and absence north of the PF, is the difference in H_4SiO_4 supply rates between the two locations. The factors controlling the supply rate of nutrients from below the mixed layer are wind-driven mixing, vertical motion driven by wind stress curl, the gradient of nutrients with depth, the depth of the mixed layer, and the strength of stratification. Since winds in this open-ocean area are associated with large-scale weather systems, wind direction and wind stress are on average uniform across our survey area (between $\sim 60^\circ$S and $\sim 62^\circ$S). However, the profiles of H_4SiO_4 on either side of the front clearly indicate a three-fold increase of the H_4SiO_4 gradient with depth south of the front (Fig. 7a–c). Despite the narrow range over which the mixed-layer depths varied within the survey area, a trend between the decrease in mixed-layer depth and an increase in the fuco (diatom) dominance can be observed (Fig. 6c and d). The coincidence of shallower mixed-layer depths and stronger vertical H_4SiO_4 gradient south of the front resulted likely in an increased flux of H_4SiO_4 to surface waters from below the mixed layer. An estimate for H_4SiO_4 eddy flux yields a flux of 1.6 mmol H_4SiO_4 $m^{-2}\,d^{-1}$ south of the PF (62°S) and 0.5 mmol H_4SiO_4 $m^{-2}\,d^{-1}$ north of the PF (60°S) (Table 1). These flux estimates would support 23% of the integrated silicic acid production measured by Brzezinski et al. (2001) at 62°S and 10% of the production estimates at 60°S.

The same calculation for iron flux yields a positive flux of iron south of the PF and a negative flux of the same magnitude north of the PF (Table 2). This would suggest that both silicic acid and iron limitation were alleviated south of the PF due to the positive flux of iron as opposed to north of the PF, where iron concentrations were diluted. However, when production rates of biogenic silicic acid were translated into biogenic iron production rates based on phytoplankton Si : Fe ratios in the literature (Collier and Edmond, 1983; Martin and Knauer, 1973; Martin et al., 1976), iron eddy flux on either side of the PF appeared negligible compared to iron necessary to sustain such production rates (ratio Fe flux : Fe production estimate = 0.0003) (Table 2). This comparison between estimated biogenic iron production rates and iron eddy fluxes suggests that even in regions of high meander-driven upwelling, iron flux from below the mixed layer was likely to be

insignificant. Based on this discrepancy in iron flux and production estimates, we conclude that differences in iron supply on either side of the PF were less likely to account for the shift to diatom dominance south of the PF than the differences in silicic acid flux estimates on either side of this front.

5. Conclusion

Although increased light availability as a result of shallower mixed layers appears to be crucial for the initiation of a bloom in spring and early summer (Mitchell and Holm-Hansen, 1991; Abbott et al., 2001; Smith et al., 2000), subsequent phytoplankton accumulation in midsummer is not correlated to mixed-layer depths (Fig. 6) and likely not a function of light availability. The observed correlation between increased diatom dominance over prymnesiophytes and shallower mixed layers is in agreement with observations made by Arrigo et al. (1999) in the Ross Sea. However, we believe that in our case this correlation does not necessarily result from increased light availability, since the scarce light data indicate that regardless of the mixed-layer depths diatoms and prymnesiophytes are both being mixed to the bottom of the euphotic zone. With the low ambient silicic acid and iron concentrations observed during this cruise, it is not surprising that we do not find a correlation with the mixed-layer concentrations but with the concentrations below the mixed layers. This is in agreement with a previous study, which observed diatom dominance coinciding with locations of upwelling during austral summer (Prézelin et al., 2000). This supports the hypothesis that the factors controlling the phytoplankton biomass shift from light limitation to silicic acid and iron limitation between austral spring and summer. Therefore, we conclude that the increased diatom dominance south of the PF is a consequence of increased silicic acid and possibly iron flux to the mixed layer. This increased flux south of the PF is possible due to the shallower mixed layer and the increased nutrient gradient with depth.

We speculate that additional meander-driven upwelling of silicic acid will further stimulate the growth of diatoms at the southern edge of the PFR, which in turn would increase the efficiency of the biological pump in exporting carbon. The significance of the meander-driven re-supply of iron to the biology is less clear, due to a lack of information on the iron requirement for Southern Ocean phytoplankton. In the subsequent downwelling region of the meander, the export of the organic material out of the upper mixed layer will be further enhanced (Flierl and Davis, 1993). This interplay between the upwelling and downwelling region of the front has the potential to contribute significantly to the export of organic carbon even after the occurrence of the bloom. This is confirmed by observations of a substantial flux ($156\,mg\,m^{-2}d^{-1}$) into a sediment trap at 1003 m below the PF (Honjo et al., 2000). Flux estimates of upwelling nutrients and downwelling biomass in terms of carbon are necessary to assess the overall importance of the PFR to the carbon budget of the Southern Ocean.

Acknowledgements

We are grateful to the captain and crew of the R/V *Roger A. Revelle* for their assistance in the collection of the data. Thanks are expressed to M.A. Brzezinski, D.M. Nelson, L.A. Codispoti

and J.M. Morrison for providing the silicic acid data and T.J. Cowles for the euphotic depth data. I would also like to acknowledge F.G. Prahl and M.A. Sparrow for their helpful suggestions and continuos support for the HPLC analysis. I especially thank D.M. Nelson for helpful comments and suggestions for the manuscript. I would also like to thank W.O. Smith and J.R. Nelson for their suggestions, which greatly improved the manuscript. This research was supported by the National Science Foundation, Office of Polar Programs Grants OPP-9530507 (M.R. Abbott and J.G. Richman) and OPP-9530758 (J.A. Barth and T.J. Cowles) and the NASA Grant NAS5-31360 (M.R. Abbott). (US JGOFS Contribution No. 616)

References

Abbott, M.R., Richman, J.G., Letelier, R.M., Bartlet, J.S., 2000. The spring bloom in the Antarctic Polar Frontal Zone as observed from a mesoscale array of bio-optical sensors. Deep-Sea Research II 47, 3285–3314.

Abbott, M.R., Richman, J.G., Nahorniat, J.S., Barksdale, B.S., 2001. Meanders in the Antarctic Polar Frontal Zone and their impact on phytoplankton. Deep-Sea Research II 48, 3891–3912.

Arrigo, K.R., Robinson, D.H., Worthen, D.L., Dunbar, R.B., DiTullio, G.R., van Woert, M., Lizotte, M.P., 1999. Phytoplankton community structure and the drawdown of nutrients and CO_2 in the Southern Ocean. Science 283, 265–267.

Banse, K., 1996. Low seasonality of low concentrations of surface chlorophyll in the Subantarctic water ring: underwater irradiance, iron, or grazing? Progress in Oceanography 37, 241–291.

Barth, J.A., Bogucki, D.J., 2000. Spectral light absorption and attenuation measurements from a towed undulating vehicle. Deep-Sea Research I 47, 323–342.

Barth, J.A., Cowles, T.J., Mesoscale physical, bio-optical structure of the Antarctic Polar Front near 170°W during austral summer, in preparation.

Barth, J.A., Cowles, T.J., Pierce, S.D., 2001. Mesoscale physical, bio-optical structure of the Antarctic Polar Front near 170°W during austral spring. Journal of Geophysical Research 106, 13 879–13 902.

Berger, W.H., Wefer, G., 1991. Productivity of the glacial ocean: discussion of the iron hypothesis. Limnology and Oceanography 36, 1899–1918.

Bidigare, R.R., Iriarte, J.L., Kang, S.-H., Karentz, D., Ondrusek, M.E., Fryxell, G.A., 1996. Phytoplankton: quantitative and qualitative assessment. In: Ross, R., Hofmann, E., Quetin, L. (Eds.), Foundations for Ecological Research West of the Antarctic Peninsula, Antarctic Research Series 70, American Geophysical Union, pp. 173–198.

Boden, T.A., Kaiser, R.J., Stepnoski, R.J., Stoss, F.W., 1994. Trends '93: A Compendium of Data on Global Change. Carbon Dioxide Information Analysis Center, Oak Ridge, p. 984.

Brainerd, K.E., Gregg, M.C., 1995. Surface mixed and mixing layer depths. Deep-Sea Research I 42, 1521–1543.

Brown, S.L., Landry, M.R., 2001. Microbial community structure and biomass in surface waters during a Polar Front summer bloom along 170°W. Deep-Sea Research II 48, 4039–4058.

Brzezinski, M.A., Nelson, D.M., 1989. Seasonal changes in the silicon cycle within a Gulf Stream warm-core ring. Deep-Sea Research 36, 1009–1030.

Brzezinski, M.A., Phillips, D.R., Chavez, F.P., Friederich, G.E., Dugdale, R.C., 1997. Silica production in the Monterey, California, upwelling system. Limnology and Oceanography 42, 1694–1705.

Brzezinski, M.A., Nelson, D.M., Franck, V.M., Sigmon, D.E., 2001. Silicon dynamics within an intense open-ocean diatom bloom in the Pacific sector of the Southern Ocean. Deep-Sea Research II 48, 3997–4018.

Buma, A.G.J., Bano, N., Veldhuis, M.J.W., Kraay, G.W., 1991. Comparison of the pigmentation of two strains of the prymnesiophyte *Phaeocystis* sp. Netherland. Journal of Sea Research 27, 173–182.

Collier, R.W., Edmond, J.M., 1983. Plankton compositions and trace element fluxes from the surface ocean. In: Trace Metals in Sea-Water. NATO Conference Series 4, Plenum Press, New York, pp. 789–809.

De Baar, H.J.W, de Jong, J.T.M, Bakker, D.C.E., Löscher, B.M., Veth, C., Bathmann, U., Smetacek, V., 1995. Importance of iron for plankton blooms and carbon dioxide drawdown in the Southern Ocean. Nature 373, 412–415.

De Baar, H.J.W., de Jong, J.T.M., Nolting, R.F., Timmermans, K.R., van Leeuwe, M.A., Bathmann, U., Rutgers van der Loeff, M., Sildam, J., 1999. Low dissolved Fe and the absence of diatom blooms in remote Pacific waters of the Southern Ocean. Marine Chemistry 66, 1–34.

Dugdale, R.C., Goering, J.J., 1967. Uptake of new and regenerated forms of nitrogen in primary productivity. Limnology and Oceanography 12, 196–207.

Dugdale, R.C., Wilkerson, F.P., Minas, H.J., 1995. The role of a silicate pump in driving new production. Deep-Sea Research I 42, 697–719.

Flierl, G.R., Davis, C.S., 1993. Biological effects of Gulf Stream meandering. Journal of Marine Research 51, 529–560.

Franck, V.M., Brzezinski, M.A., Coale, K.H., Nelson, D.M., 2000. Iron and silicic acid concentrations regulate Si uptake north and south of the Polar Frontal Zone in the Pacific Sector of the Southern Ocean. Deep-Sea Research II 47, 3315–3338.

Fryxell, G.A., Kendrick, G.A., 1988. Austral spring microalgae across the Weddell Sea ice edge: spatial relationships found along a northward transect during AMERIEZ 83. Deep-Sea Research I 35, 1–20.

Holm-Hansen, O., El-Sayed, S.Z., Franceschini, G.A., 1977. Primary production and the factors controlling phytoplankton growth in the Southern Ocean. In: Adaptations within Antarctic Ecosystems. Proceedings of the Third SCAR Symposium on Antarctic Biology, pp. 11–50.

Honjo, S., Francois, R., Manganini, S., Dymond, J., Collier, R., 2000. Particle fluxes to the interior of the Southern Ocean in the Western Pacific sector along 170°W. Deep-Sea Research II 47, 3521–3548.

Jeffrey, S.W., Vesk, M., 1997. Introduction to marine phytoplankton and their pigment signatures. In: Jeffrey, S.W., Mantoura, R.F.C., Wright, S.W. (Eds.), Phytoplankton pigments in oceanography: guidelines to modern methods. UNESCO Publishing, Paris, pp. 37–84.

Jeffrey, S.W., Sielicki, M., Haxo, F.T., 1975. Chloroplast pigment patterns in dinoflagellates. Journal of Phycology 11, 374–384.

Jeffrey, S.W., Mantoura, R.F.C., BjØrnland, T., 1997. Data for the identification of 47 key phytoplankton pigments. In: Jeffrey, S.W., Mantoura, R.F.C., Wright, S.W. (Eds.), Phytoplankton pigments in oceanography: guidelines to modern methods. UNESCO Publishing, Paris, pp. 449–559.

JGOFS, 1996. Protocols for the Joint Global Ocean Flux Study (JGOFS) Core Measurements. Report No. 19, Intergovernmental Oceanographic Commission, Bergen, Norway.

Keeling, R.F., Piper, S.C., Heimann, M., 1996. Global and hemispheric CO_2 sinks deduced from changes in atmospheric O_2 concentration. Nature 381, 218–2221.

Knox, F., McElroy, M.B., 1984. Changes in atmospheric CO_2: influence of the marine biota at high latitude. Journal of Geophysical Research 89, 4629–4637.

Landing, W.M., Haraldson, C., Paxeus, J., 1986. Vinyl polymer agglomerate based transition metal cation chelating ion-exchange resin containing 8-hydroxyquinoline functional group. Analytical Chemistry 58, 3031–3035.

Longhurst, A.R., 1991. Role of the marine biosphere in the global carbon cycle. Limnology and Oceanography 36, 1507–1526.

Martin, J.H., Knauer, G.A., 1973. The elemental composition of plankton. Geochimica et Cosmochimica Acta 37, 1639–1653.

Martin, J.H., Bruland, K.W., Broenkow, W.W., 1976. Cadmium transport in the California Current. In: Windom, H., Duce, R. (Eds.), Marine pollutant transfer. Heath, Lexington, MA, pp. 159–184.

Martin, J.H., Gordon, R.M., Fitzwater, S.E., 1990. Glacial-interglacial CO_2 change: the iron hypothesis. Paleoceanography 5, 1–13.

Measures, C.I., Yuan, J., Resing, J.A., 1995. Determination of iron in seawater by flow injection analysis using in-line preconcentration and spectrophotometric detection. Marine Chemistry 50, 3–12.

Mitchell, B.G., Holm-Hansen, O., 1991. Observations and modeling of the Antarctic phytoplankton crop in relation to mixing depth. Deep-Sea Research I 38, 981–1007.

Moore, J.K., Abbott, M.R., 2000. Phytoplankton chlorophyll distributions and primary production in the Southern Ocean. Journal of Geophysical Research—Oceans 105, 28 709–28 722.

Moore, J.K., Abbott, M.R., Richman, J.G., 1999. Location and dynamics of the Antarctic Polar Front from satellite sea surface temperature data. Journal of Geophysical Research 104, 3059–3073.

Nelson, D.M., Smith, W.O., 1991. Sverdrup revisited: critical depths, maximum chlorophyll levels, and the control of Southern Ocean productivity by the irradiance-mixing regime. Limnology and Oceanography 36, 1650–1661.

Nelson, D.M., McCarthy, J.J., Joyce, T.M., Ducklow, H.W., 1989. Enhanced near-surface nutrient availability and new production resulting from the frictional decay of a Gulf Stream warm-core ring. Deep-Sea Research I 36, 705–714.

Nelson, D.M., Brzezinski, M.A., Sigmon, D.E., Franck, V.M., 2001. Direct kinetic evidence of Si limitation in the Pacific sector of the Southern Ocean during austral spring and summer, 1997–1998. Deep-Sea Research II, submitted.

Orsi, A.H., Whitworth III, T., Nowlin Jr., W.D., 1995. On the meridional extent and fronts of the Antarctic Circumpolar Current. Deep-Sea Research I 42, 641–673.

Peng, T.-H., Broecker, W.S., 1991. Factors limiting the reduction of atmospheric CO_2 by iron fertilization. Limnology and Oceanography 36, 1919–1927.

Prézelin, B.B., Hofmann, E.E., Mengelt, C., Klinck, J.M., 2000. The linkage between Upper Circumpolar Deep Water (UCDW) and phytoplankton asse mblages on the west Antarctic Peninsula continental shelf. Journal of Marine Research 58, 165–202.

Sarmiento, J.L., Orr, J.C., 1991. Three-dimensional simulations of the impact of Southern Ocean nutrient depletion on atmospheric CO_2 and ocean chemistry. Limnology and Oceanography 36, 1928–1950.

Smith, W.O., Nelson, D.M., 1985. Phytoplankton bloom produced by a receding ice edge in the Ross Sea: spatial coherence with the density field. Science 277, 163–166.

Smith, W.O., Nelson, D.M., 1990. Phytoplankton growth and new production in the Weddell Sea marginal ice zone in the austral spring and autumn. Limnology and Oceanography 35, 809–821.

Smith, W.O., Anderson, R.F., Moore, J.K., Codispoti, L.A., Morrison, J.M., 2000. The US Southern Ocean Joint Global Flux Study: an introduction to AESOPS. Deep-Sea Research II 47, 3073–3093.

Tréguer, P., Jacques, G., 1992. Dynamics of nutrients and phytoplankton, and fluxes of carbon, nitrogen and silicon in the Antarctic Ocean. Polar Biology 12, 149–162.

Vaulot, D., Birrien, J.L, Marie, D., Casotti, R., Veldhuis, M.J.W., Kraay, G.W., Chretiennot-Dinet, M.-J., 1994. Morphology, ploidy, pigment composition, and genome size of cultured strains of *Phaeocystis* (Prymnesiophyceae). Journal of Phycology 30, 1022–1035.

Vink, S., Boyle, E.D., Yuan, J.C., Measures, C.I., 2000. Automated high resolution determination of the trace elements iron and aluminum in the surface ocean using a towed fish coupled to flow injection analysis. Deep-Sea Research I 47, 1141–1156.

Wright, S.W., Jeffrey, S.W., 1987. Fucoxanthin pigment markers of marine phytoplankton analyzed by HPLC and HPTLC. Marine Ecology Progress Series 38, 259–266.

Wright, S.W., Jeffrey, S.W., 1997. High-resolution HPLC system for chlorophylls and carotenoids of marine phytoplankton. In: Jeffrey, S.W., Mantoura, R.F.C., Wright, S.W. (Eds.), Phytoplankton pigments in oceanography: Guidelines to modern methods. UNESCO Publishing, Paris, pp. 327–341.